Thesis for the Degree of Master of Engineering

A Study of Controlling a Tricopter

by

Giang Hoang

Department of Interdisciplinary Program of

Mechatronics Engineering, The Graduate School,

Pukyong National University

February 2011

A Study of Controlling a Tricopter

3개의 회전날개를 가진 헬리콥터 제어에 대한 연구

Advisor: Prof. Sang Bong Kim

by

Giang Hoang

A thesis submitted in partial fulfillment of the requirements
for the degree of

Master of Engineering

in Department of Interdisciplinary Program of Mechatronics Engineering,
The Graduate School,
Pukyong National University

February 2011

A Study of Controlling a Tricopter

A dissertation

by

Giang Hoang

Approved by:

Prof. Ill Yeong Lee

(Chairman) ______________________

Prof. In Pil Kang

(Member) ______________________

Prof. Sang Bong Kim

(Member) ______________________

December 2011

Acknowledgements

At first, I am deeply grateful to my supervisor, Professor Sang Bong Kim, for his valuable advice, guidance and support during the process of my studying in Korea. He has been providing a large amount of knowledge, the direction and skill of research, and strong motivation for my researching. His kindness, insight and continuous supports encouraged and helped me to accomplish my research and finish this dissertation scientifically.

I would like to thank the members of my thesis committee: Prof. Ill Yeong Lee and Prof. In Pil Kang for their considerable helpful comments and suggestions.

I would like to thank Prof. Hak Kyeong Kim for his great helps to research and complete this thesis. I could not finish my dissertation on time without his great help.

I am grateful to Dr. Tan Tien Nguyen and Dr. Thien Phuc Tran from Ho Chi Minh City University of Technology for their essential assistances.

I would like to thank all members of CIMEC laboratory for their cooperation and for all the kindness and friendship, Mr. Nak Soon Choi, Mr. Do Kyoung Lee, Mr. Dae Won Kim, Mr. Dae Hwan Kim, Mr. Chul Han Park, Mr. Kyeong Mok Lee, Mr, Viet Tuan Dinh, Mr. Phuc Thinh Doan, Mr. Seo Kwang Kim, Miss. Yu Mi Park, Miss. Min Ji Bae, Mr. Woo Yeung Jung, Mr. Sang Jin Han for all scientific discussions and helps.

Thanks are due to all members of Vietnamese Student's Association in Korea, especially Mr. Manh Vu Tran, Mr. Van Phuoc

Bui, Mr. Hong Thom Pham, Mr. Thank Khoa Phung, Mr. Phuoc Hoang Ho, Mr. Hong Duc Pham and Ms. Thanh Xuan Phung for their vigorous support.

Finally, I would like to thank to my father, my mother, my sister and all my close relatives for their love, endless encouragement for me not only in the dissertation time but also in the whole of my life.

Busan, December 15, 2011

Giang Hoang

Contents

A study of Controlling a Tricopter

Hoang Giang

Department of Interdisciplinary program of Mechatronics Engineering,
The Graduate School, Pukyong National University

Abstract

The objective of this dissertation is about the study on controlling a three rotor helicopter or a tricopter. The tricopter is an aircraft with two fixed rotors and one tilting rotor. In this dissertation, the following three problems are considered. The first one is the kinematic and dynamic modellings of a tricopter. The second is control algorithm. The last one is hardware development.

First, the kinematic and dynamic modellings of the tricopter are presented to understand its behavior. The Newton-Euler formula and the Euler angles theories are used to provide the modellings information with physics and mathematical derivatives. The dynamic modelling is linearized to reduce its complexity. The outputs chosen are the Euler angles (attitude or orientation) and the height (attitude) of the tricopter.

Second, a controller to control the altitude and attitude separately is proposed. From the linearized dynamic model and the control strategy, a tracking controller is designed using the backstepping control algorithm. The objective of the controller is to make the outputs converge to the references inputs.

Third, to implement the proposed tracking controller, a real tricopter platform is developed with several interconnected devices such as: motors, sensors, Micro Control Unit (MCU), etc. The sensors are used for measuring the aircraft attitude and its height from the ground. The sensors' data and the control algorithm are computed by the Micro National Control Unit (MCU) which provides the signals to the motors.

Finally, simulation results are done to demonstrate the effectiveness of the proposed controller.

Keywords: Aero Dynamic, Unmanned Aerial Vehicles (UAVs), Vertical Take Off and Land (VTOL), Backstepping Control

List of Figures

List of Tables

Chapter 1: Introduction

1.1 Background and motivation

In recent years, a growing interest has been shown in unmanned aerial vehicles (UAVs) defined as non-pilot flying vehicles. These air machines are either remotely controlled or operate automatically. In fact, many civil and military applications need the capabilities of UAVs [22~24]. They open up applications in the fields of security (supervision of aerial space), management of natural ricks (supervision of active volcanoes), environment (measuring air pollution), agriculture (detection and of infested cultivations). In Fig. 1, UAVs are used for gathering information in desert and hurricane. The UAV Eagle Eye shown in Fig. 2 is used to support maritime security, search and rescue missions, etc. UAVs are expected to be a major part of the aviation industry over next few years with the improvements in computer science, electronics, communication, sensors, etc.

Fig. 1.1 Investigating UAVs

Fig. 1.2 UAV Eagle Eye

In UAVs field, the rotary-wing UAVs have many advantages with the capabilities of VTOL (Vertical Take-off and Landing), omni-directional flying and hovering performance. Design of UAVs involves many problems related to limited payload, energy consumption, navigation, etc. Several structures and configurations have been developed, for example, classical helicopters [25], two-tilting rotor aircraft[9], four rotor aircraft[1~4], three rotors aircraft[5~6], six rotor aircraft[6], eight rotor aircraft[7, 37], etc. Each of them has advantages and drawbacks. A classical helicopter has a main rotor, which provides the total thrust, and a tail rotor for compensating the reactive anti-torque due to the main rotor. The lateral force generated by the tail rotor is used for yaw angle control and does not participate in the total thrust generation. So the energy spent as the tail rotor can be considered as a lost energy. The blades on a helicopter main rotor are angled in different ways by two servomotors to control the orientation and direction of the aircraft. The advantage of these helicopters is to have the good performance during forward flight. But the classical helicopter has many mechanical linkages and swashplate makes it difficult to control or repair. The four rotors aircraft is characterized with four rotors in a cross configuration. The front and the rear propellers rotate counter-clockwise, while the left and the right ones turn clockwise. This configuration removes the need of a tail rotor or any servomechanism. All rotors participate to provide the main thrust. The control torques are generated by the four rotors. The yaw torque of this aircraft is obtained by increasing (or decreasing) the speed of the front-rear rotors and decreasing (or increasing) the speed of the left-right rotors. The yaw torque modeling is complex due to the aero-dynamical relations. And the main drawback is the high energy consumption with four rotors.

Since these advantages and drawbacks are due to characteristics of the aircrafts, the three rotors aircraft or tricopter which presents a good trade-off between conventional helicopter and four rotor aircraft has been chosen for this dissertation. Three rotor aircraft's mechanical structure is as simple as the four rotor aircrafts'. It can reduce one motor than the four rotors aircraft.

The stabilization control problem of rotary-wing UAVs is challenging since their dynamics are highly nonlinear and coupled with unknown disturbance. The control of a rotorcraft in hovering has been researched with different techniques. In [7], H. Romero et al. proposed an original configuration of an eight rotor UAV using PD control. The eight rotor rotorcraft is simpler to pilot than other rotorcraft, but it consumes a lot of energy with eight rotors. R. Lozano et al. [4] proposed a stabilization control for a mini rotorcraft with four rotors based on nested saturations. They guaranteed the asymptotical stability of the helicopter. In [9], F. Kendoul et al. presented the hover control of a two-tilting rotors VTOL aircraft. The dynamic model of this aircraft is complex. The controller based on the backstepping method. The convergence of the rotorcraft internal states is guaranteed, but pitch angle result in simulation still oscillates. The PD^2 feedback and PID controller also can be used to control the rotorcraft [20, 27~28]. The PID controller does not require some specific model parameters and is simple to implement. But the controller provided average results due to the model imperpections. The PD^2 feedback technique has the exponential convergence property by compensating the Coriolis and gyroscopic terms. But the experiment results did not make much difference compared to traditional PD control. In [29], Y. Morel et al. used the adaptive control for a quadrotor. This method provides good performance with parameters uncertainties. But the controller is complex and there are no experiment results. In [30~31], the dynamic feedback technique is used to transform the quadrotor system into linear controllable subsystems. From the simulation results, the feedback linearization control is not robust enough to control the outputs of the quadrotor because the feedback linearization method does not reflect the nonlinear system. Another control is based on visual feedback by a camera which can be mounted on-board or fixed on the ground [32~34]. The main drawback of this controller is to need enough light to work properly. Artificial controllers also have been used in UAVs field such as fuzzy techniques, neural networks[35~36]. But their controller was still not effective, the angle simulation results showed the chattering behavior. In [5], S. Salazar-Cruz et al. presented the design and control algorithm of tricopter. Their controller was based on the sum of saturating functions also has to consider the inputs boundedness.

To solve above problems, with the inputs boundedness, the dynamic model of the helicopter can be linearized to simplify the system to be controlled. Therefore, the controller based on the linearized dynamic model is considered in this dissertation. The tricopter with the combination of the advantages of conventional helicopters and quadrotor is chosen as flying platform for this disseration. And a controller with a strategy to make the tricopter able to act as a conventional helicopter is needed deeply.

1.2 Objective and researching method of this dissertation

From the above discussions, the purpose of this dissertation is modeling and controlling a tricopter. The goals of this dissertation are the system modeling, the control algorithm design and the simulation and experiment to evaluate the designed controller.

The tricopter's modeling is derived with physics and mathematical derivations. Newton-Euler formula and the Euler angles theories are chosen to derive the kinematic and dynamic equations. These equations are very important because they describe the behavior of tricopter according to the inputs.

After the modeling system is achieved, the dynamics model is linearized to reduce the algorithm complexity. The Euler angles (altitude or orientation) and the high (attitude) of the tricopter are chosen as the outputs to be controlled. A controller to control the altitude and attitude separately is proposed to reduce the effect of the centrifugal terms. The controller is designed by backstepping method. The effectiveness of the tricopter dynamic model and the designed controller are verified by simulation results.

The real tricopter platform is developed by creating a system of interconnected devices such as motors, sensors, MCU, etc. Two types of sensors are used for measuring attitude and altitude of the tricopter. For measuring attitude, gyros, accelerometers and compass sensors are fused by a discrete recursive complementary filter. The Micro Control Unit (MCU) handles sensors signals, control algorithm and provides the signals to the rotors. The simulation results are done to verify the effectiveness of the proposed controller.

1.3 Outline of dissertation and summary of contributions

Chapter 1: Introduction

In this chapter, background and motivation of the three rotors aircraft system is described. Objective and researching method of this dissertation are presented. And the outline of content and summary of contribution of this dissertation is given.

Chapter 2: System modeling

This chapter provides the derivation of the three rotors aircraft model. The modeling of kinematic and dynamic of the three rotors aircraft is presented based on the Newton-Euler formalism. This chapter consists four sections. The first section is about basic concepts of three rotors aircraft. The kinematic and dynamic models are presented in the second and third section, respectively. And the system architecture is provided in the last chapter.

Chapter 3: Controller design

This chapter focuses on the control algorithm needed to stabilize the tricopter. There are two sections in this chapter. In the first section, the model of the tricopter is simplified to be easier to control and to reduce the algorithm calculation. The backstepping techniques is adopted to control the tricopter and provided in the second chapter.

Chapter 4: Hardware and software design

The hardware structure of the tricopter system is describes in this chapter. This chapter has two sections. The first section presents the hardware configuration of the control system including motors, sensors, MCU, etc. And the second one is the software development. The program structure of the MCU to filter the sensors data and compute the algorithm is presented in this section.

Chapter 5: Simulation results

Simulation results are given to show the effectiveness of the proposed controller.

Chapter 6: Conclusions and Future Work

Conclusions for this dissertation and some ideas for future work are presented.

Chapter 2: System modeling

2.1 Basic concepts and system description of tricopter

The tricopter consists of two body-fixed rotors and a tail tilting rotor. The two front rotors rotate in the opposite directions, the left one rotates counter-clockwise, while the right one turns clockwise. Therefore, reactive anti-torques of each rotor are eliminated. The tail rotor rotates clockwise. Therefore, without tilting tail rotor, the whole system tends to have a yawing moment in the counterclockwise directions, and this is the reason for having a servo motor on the tail rotor axis for tilting purposes. As the tail rotor tilts, it creates a moment that cancels the yawing moment of the system.

The tricopter motion can be decomposed into 4 basic movements which allow the tricopter to reach a certain height and attitude. These basic movements can be described by the following commands:

- Throttle: this command is provided by increasing (or decreasing) all the rotors' speed by the same amount. A total thrust is generated to raise or lower the tricopter when the tricopter is in horizontal position. Otherwise, the provided thrust makes the tricopter move left (right) or forward (backward) based on the angular position of the tricopter.
- Roll: this command is provided by increasing (or decreasing) the left rotor and decreasing (or increasing) the right one while keeping the total thrust the same. It leads to a torque

with respect to (WRT) the $\overrightarrow{O_B x_B}$ axis in Fig. 2.1 that generates roll rotation acceleration.

- Pitch: this command is provided by increasing (or decreasing) two front rotors and decreasing (or increasing) the tail rotor while keeping the total thrust the same. It leads to a torque with respect to the $\overrightarrow{O_B y_B}$ axis in Fig. 2.1 which generates pitch rotation acceleration.
- Yaw: this command is provided by using the natural yawing movement from the reaction torque and also from the tilt angle of the tail rotor. The yaw torque is a sum of the reaction torque and the vertical part of the force generated by the tail rotor.

Fig 2.1 shows the tricopter frame system.

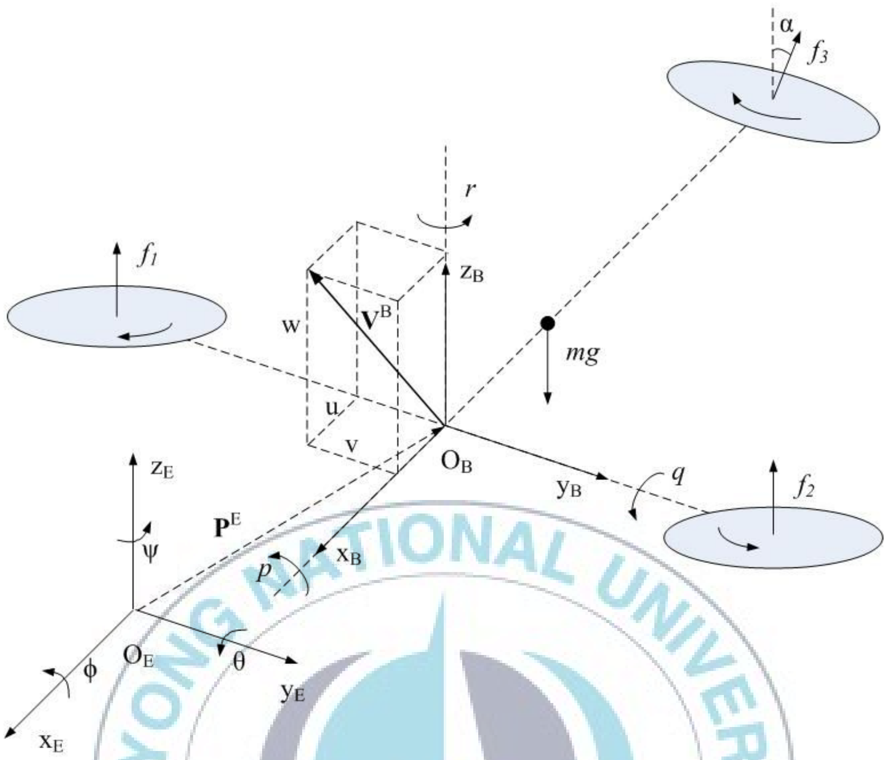

Fig. 2.1 Tricopter frame system

The symbols used for describing frame system of the tricopter are shown in Table 2.1.

Table 2-1 Symbols for describing frame system of the tricopter

Symbol	Definition
x	tricopter linear position along $\overrightarrow{O_E x_E}$ axis WRT E-frame
y	tricopter linear position along $\overrightarrow{O_E y_E}$ axis WRT E-frame
z	tricopter linear position along $\overrightarrow{O_E z_E}$ axis WRT E-frame
ϕ	tricopter angular position around $\overrightarrow{O_E x_E}$ axis WRT E-frame
θ	tricopter angular position around $\overrightarrow{O_E y_E}$ axis WRT E-frame
ψ	tricopter angular position around $\overrightarrow{O_E z_E}$ axis WRT E-frame

u	tricopter linear velocity along $\overrightarrow{O_B x_B}$ axis WRT B-frame
v	tricopter linear velocity along $\overrightarrow{O_B y_B}$ axis WRT B-frame
w	tricopter linear velocity along $\overrightarrow{O_B z_B}$ axis WRT B-frame
p	tricopter angular velocity around $\overrightarrow{O_B x_B}$ axis WRT B-frame
q	tricopter angular velocity around $\overrightarrow{O_B y_B}$ axis WRT B-frame
r	tricopter angular velocity around $\overrightarrow{O_B z_B}$ axis WRT B-frame
α	tilt angle of the tail rotor

2.2 Modelling of tricopter

The aircraft dynamics and kinematics in three-dimensional space can be described by a set of differential equations which identifies a 6 degree of freedom (DOF) rigid body. The Newton-Euler is adopted in this work. In this chapter, the tricopter system is modeled according to two parts:

- Kinematics
- Dynamics

2.2.1 Kinematic modelling

At first, we overview the coordinate systems that are used as the reference frame for the description of the tricopter motion. To define the motion of a six DOF rigid body, it is usual to use two reference frames:

- Earth inertial reference (E-frame)
- Body-fixed reference (B-frame)

In Fig. 2.1, the E-frame (O_E, x_E, y_E, z_E) is a Cartesian coordinate. $\overrightarrow{O_E x_E}$ points toward the North, $\overrightarrow{O_E y_E}$ points toward the West and $\overrightarrow{O_E z_E}$ points upwards. This frame is used to define the linear position vector ($\mathbf{P}^E = \begin{bmatrix} x & y & z \end{bmatrix}^T$) and the angular position vector ($\mathbf{A}^E = \begin{bmatrix} \phi & \theta & \psi \end{bmatrix}^T$) WRT E-frame of the tricopter.

The B-frame (O_B, x_B, y_B, z_B) is attached to the body of the tricopter. The origin O_B is located at the middle point between the left rotor and the right rotor. $\overrightarrow{O_B x_B}$ to the opposite direction to tail rotor, $\overrightarrow{O_B y_B}$ toward the left rotor, and $\overrightarrow{O_B z_B}$ upwards. This frame is used to define the linear velocity vector ($\mathbf{V}^B = \begin{bmatrix} u & v & w \end{bmatrix}^T$) and the angular velocity vector ($\mathbf{\Omega}^B = \begin{bmatrix} p & q & r \end{bmatrix}^T$) WRT B-frame of the tricopter.

The linear position vector, $\mathbf{P}^E$,of the tricopter is the position vector of the origin of the B-frame WRT E-frame. And the angular position vector (or attitude), $\mathbf{A}^E$, of the tricopter is defined by the orientation of the B-frame WRT E-frame. This is given by three rotations about the main axes which take the E-frame into the B-frame. The rotation matrix, $\mathbf{R}_B^E$, represents a rotational transformation between the E-frame and B-frame, and is obtained by post-multiplying the three basic rotation matrices as follows:

- Rotation matrix about the z_E axis of the angle ψ (yaw) as shown in Fig. 2.2 is denoted as $\mathbf{R}(\psi, z_E)$.

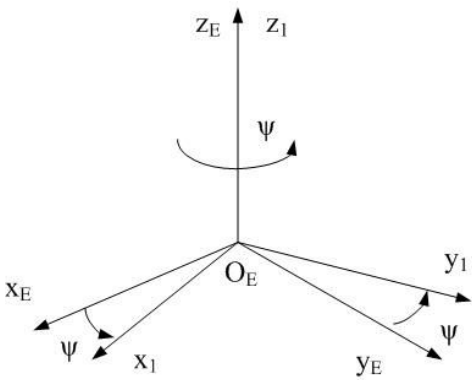

Fig. 2.2 Rotation around the z_E axis

Denoting $\mathbf{V}^E$ is the linear velocity vector of the tricopter WRT the E-frame, $\mathbf{V}^E$ is obtained as follows:

$$\mathbf{V}^E = \mathbf{R}(\psi, z_E)\mathbf{V}^1 = \mathbf{R}_1^E\mathbf{V}^1 \tag{2.1}$$

where $\mathbf{V}^1$ is a representation of $\mathbf{V}^E$ in the current frame (O_E, x_1, y_1, z_1).

The rotation matrix, $\mathbf{R}_1^E = \mathbf{R}(\psi, z_E)$, represents a rotational transformation between the E-frame and (O_E, x_1, y_1, z_1), is presented as follows:

$$\mathbf{R}_1^E = \begin{bmatrix} \vec{i}_1 \cdot \vec{i}_E & \vec{j}_1 \cdot \vec{i}_E & \vec{k}_1 \cdot \vec{i}_E \\ \vec{i}_1 \cdot \vec{j}_E & \vec{j}_1 \cdot \vec{j}_E & \vec{k}_1 \cdot \vec{j}_E \\ \vec{i}_1 \cdot \vec{k}_E & \vec{j}_1 \cdot \vec{k}_E & \vec{k}_1 \cdot \vec{k}_E \end{bmatrix} = \begin{bmatrix} c_\psi & -s_\psi & 0 \\ s_\psi & c_\psi & 0 \\ 0 & 0 & 1 \end{bmatrix} \tag{2.2}$$

where $\vec{i}_1$, $\vec{j}_1$, $\vec{k}_1$ are unit vectors of the current frame (O_E, x_1, y_1, z_1) codirectional with the x_1 , y_1 and z_1 axes, $\vec{i}_E, \vec{j}_E, \vec{k}_E$ are unit vectors of the E-frame codirectional with the x_E , y_E and z_E axes.

- Rotation matrix about the y_1 axis of the angle θ (pitch) as shown in Fig. 2.3 is denoted as $\mathbf{R}(\theta, y_1)$.

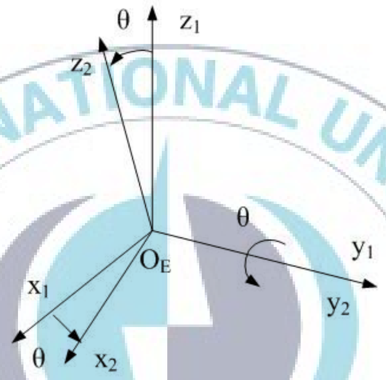

Fig. 2.3 Rotation around the y_1 axis

$$\mathbf{V}^1 = \mathbf{R}(\theta, y_1)\mathbf{V}^2 = \mathbf{R}_2^1\mathbf{V}^2 \tag{2.3}$$

where $\mathbf{V}^2$ is a representation of $\mathbf{V}^E$ in the current frame (O_E, x_2, y_2, z_2)

The rotation matrix, $\mathbf{R}_2^1 = \mathbf{R}(\theta, y_1)$, represents a rotational transformation between two frames (O_E, x_1, y_1, z_1) and (O_E, x_2, y_2, z_2), is presented as follows:

$$\mathbf{R}_2^1 = \begin{bmatrix} c_\theta & 0 & s_\theta \\ 0 & 1 & 0 \\ -s_\theta & 0 & c_\theta \end{bmatrix} \tag{2.4}$$

- Rotation matrix about the x_2 axis of the angle ϕ (roll) as shown in Fig. 2.4 is denoted as $\mathbf{R}(\phi, x_2)$.

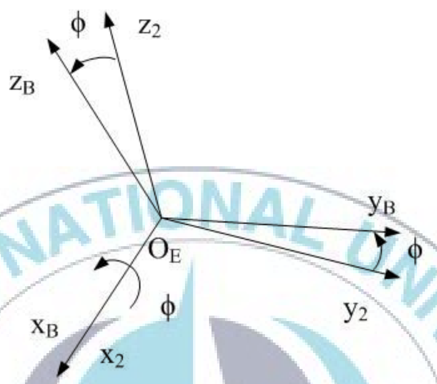

Fig. 2.4 Rotation around the x_2 axis

$$\mathbf{V}^2 = \mathbf{R}(\phi, x_2)\mathbf{V}^B = \mathbf{R}_B^2 \mathbf{V}^B \tag{2.5}$$

where $\mathbf{V}^B$ is a representation of $\mathbf{V}^B$ in the current frame (O_E, x_B, y_B, z_B).

The rotation matrix, $\mathbf{R}_B^2 = \mathbf{R}(\phi, x_2)$, represents a rotational transformation between two frames (O_E, x_1, y_1, z_1) and B-frame, is presented as follows:

$$\mathbf{R}(\phi, x_2) = \begin{bmatrix} 1 & 0 & 0 \\ 0 & c_\phi & -s_\phi \\ 0 & s_\phi & c_\phi \end{bmatrix} \tag{2.6}$$

The relation between the linear velocity vector WRT the E-frame, $\mathbf{V}^E$, and the linear velocity vector WRT B-frame, $\mathbf{V}^B$, can be presented as follows:

$$\mathbf{V}^E = \mathbf{R}_2^E \mathbf{R}_1^2 \mathbf{R}_B^1 \mathbf{V}^B = \mathbf{R}_B^E \mathbf{V}^B \tag{2.7}$$

The rotation matrix, $\mathbf{R}_B^E$, can be composed as follows:

$$\begin{aligned}\mathbf{R}_B^E &= \mathbf{R}_2^E \mathbf{R}_1^2 \mathbf{R}_B^1 = \mathbf{R}(\psi, z_E)\mathbf{R}(\theta, y_1)\mathbf{R}(\phi, x_2) = \\ &= \begin{bmatrix} c_\psi c_\theta & -s_\psi c_\phi + c_\psi s_\theta s_\phi & s_\psi s_\phi + c_\psi s_\theta c_\phi \\ s_\psi c_\theta & c_\psi c_\phi + s_\psi s_\theta s_\phi & -c_\psi s_\phi + s_\psi s_\theta c_\phi \\ -s_\theta & c_\theta s_\phi & c_\theta c_\phi \end{bmatrix}\end{aligned} \tag{2.8}$$

The notations in Eq. (2.8) are adopted as: $c_k = \cos k$, $s_k = \sin k$, $t_k = \tan k$ (where $k = \phi, \theta, \psi$).

From Eq. (2.7), the linear velocity vector WRT the E-frame, $\mathbf{V}^E$, can be presented as follows:

$$\mathbf{V}^E = \dot{\mathbf{P}}^E = \mathbf{R}_B^E \mathbf{V}^B \tag{2.9}$$

It is possible to relate the angular velocity in the E-frame to the angular velocity in the B-frame through the transformation matrix, **T**. The transformation matrix, **T,** can be determined as follows:

$$\mathbf{\Omega}^B = \begin{bmatrix} p \\ q \\ r \end{bmatrix} = \begin{bmatrix} \dot{\phi} \\ 0 \\ 0 \end{bmatrix} + \mathbf{R}(\phi, x_E)^{-1} \begin{bmatrix} 0 \\ \dot{\theta} \\ 0 \end{bmatrix} + \\ + \mathbf{R}(\phi, x_E)^{-1} \mathbf{R}(\theta, y_E)^{-1} \begin{bmatrix} 0 \\ 0 \\ \dot{\psi} \end{bmatrix} = \mathbf{T}^{-1} \begin{bmatrix} \dot{\phi} \\ \dot{\theta} \\ \dot{\psi} \end{bmatrix} \tag{2.10}$$

$$\mathbf{T}^{-1} = \begin{bmatrix} 1 & 0 & -s_\theta \\ 0 & c_\phi & c_\theta s_\phi \\ 0 & -s_\phi & c_\theta c_\phi \end{bmatrix}, \mathbf{T} = \begin{bmatrix} 1 & s_\phi t_\theta & -c_\phi t_\theta \\ 0 & c_\phi & -s_\phi \\ 0 & -s_\phi / c_\theta & c_\phi / c_\theta \end{bmatrix}$$

where $\mathbf{R}(\phi, x_E)$ is rotation matrix about the x_E axis of the angle ϕ and $\mathbf{R}(\theta, y_E)$ is rotation matrix about the x_E axis of the angle θ.

The angular velocity vector of the tricopter in the B-frame can be expressed as follows:

$$\mathbf{\Omega}^B = \mathbf{T}^{-1} \dot{\mathbf{A}}^E \tag{2.11}$$

2.2.2 Dynamic modelling

The symbols used to model the dynamics of the tricopter are shown in Table 2.2.

Table 2-2 Symbols used in dynamics of the tricopter

Symbol	Definition
$\mathbf{F}^B$	forces vector generated by rotors WRT B-frame
$\boldsymbol{\tau}^B$	torques vector generated by rotors WRT B-frame
$\mathbf{J}$	inertial matrix expressed in B-frame

f_i	force of rotor i
k_f	positive constant characterizing the propeller aerodynamics
k_τ	positive constant characterizing reactive torque
ω_i	angular velocity of rotor i
m	total mass of the tricopter
I_{xx}	moment of inertia aroung the x-axis
I_{yy}	moment of inertia aroung the y-axis
I_{zz}	moment of inertia aroung the z-axis

with $i = 1,2,3$.

The dynamics of the tricopter includes the study of forces and torques that cause the motion of the tricopter. The equations of motion for a rigid body are given by the following Newton-Euler equations in B-frame.

$$\begin{aligned} m\dot{\mathbf{V}}^B + \mathbf{\Omega}^B \times m\mathbf{V}^B &= \mathbf{F}^B \\ \mathbf{J}\mathbf{\Omega}^B + \mathbf{\Omega}^B \times \mathbf{J}\mathbf{\Omega}^B &= \boldsymbol{\tau}^B \end{aligned} \tag{2.12}$$

where $\mathbf{J} = diag(I_{xx}, I_{yy}, I_{zz})$.

Fig 2.5 shows the forces on the tricopter WRT B-frame.

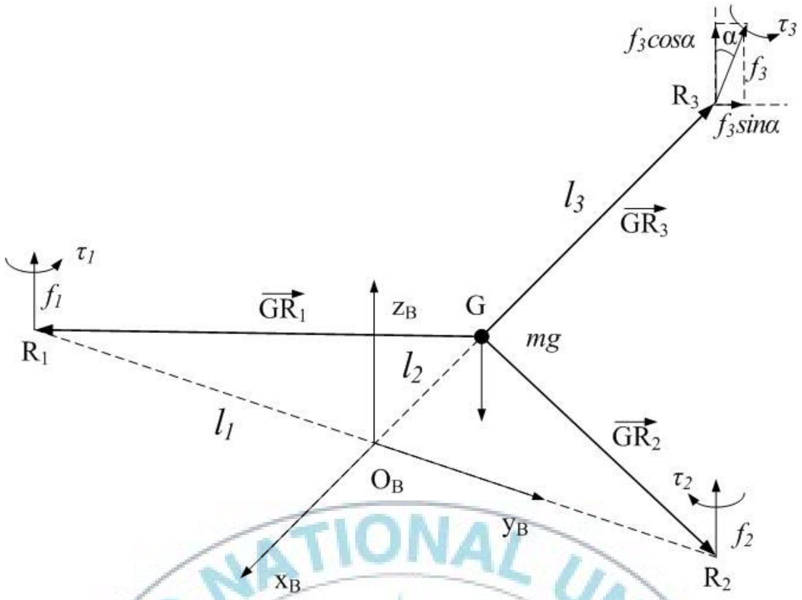

Fig. 2.5 Forces on the tricopter WRT B-frame

From Fig. 2.5, the force vector generated by rotors is expressed in B-frame as:

$$\mathbf{F}^B = \begin{bmatrix} 0 & -f_3 \sin\alpha & f_1 + f_2 + f_3 \cos\alpha \end{bmatrix}^T \tag{2.13}$$

R_1, R_2, R_3 are denoted as the applying points of the forces f_1, f_2, f_3 respectively. Then, the torque vector caused by these forces WRT the mass center G can be expressed in B-frame as follows:

$$\begin{aligned}\boldsymbol{\tau}^B = \overrightarrow{GR_1} \times (0, 0, f_1) + \overrightarrow{GR_2} \times (0, 0, f_2) \\ + \overrightarrow{GR_3} \times (0, f_3 \sin\alpha, f_3 \cos\alpha)\end{aligned} \tag{2.14}$$

where symbol × is the cross product operation on two vector with three dimensions. Counter-clockwise is chosen the positive direction.

From Eq. (2.14), the torque vector on tricopter in B-frame can be expressed as follows:

$$\boldsymbol{\tau}^B = \begin{bmatrix} \tau_\phi \\ \tau_\theta \\ \tau_\psi \end{bmatrix} = \begin{bmatrix} (f_2 - f_1)l_1 \\ f_3 l_3 \cos\alpha - (f_1 + f_2)l_2 \\ -f_3 l_3 \sin\alpha \end{bmatrix} \tag{2.15}$$

where $l_1 = \overline{O_B R_1} = \overline{O_B R_2},\ l_2 = \overline{O_B G},\ l_3 = \overline{GR_3}$ and $f_i = k_f \omega_i^2$.

The proof of Eq. (2.15) is in Appendix A.

According to the Newton third law, the rotating rotor creates reactive torque in the opposite direction. If the rotor rotates clockwise, the reactive torque makes the tricopter rotate counter-clockwise. Therefore, the main purpose of the tail rotor is to compensate for the reactive torque about *z* axis.

The front right rotor and the tail rotor rotate clockwise, the front left rotor rotates counter-clockwise. Therefore, without tilting tail rotor, the tricopter tends to have a yawing movement in counter-clockwise. The torque about *z* axis is rewritten as follows:

$$\tau_\psi = -f_3 l_3 \sin\alpha + \tau_3 \cos\alpha - \tau_2 + \tau_1 \tag{2.16}$$

The torque vector and force vector on tricopter in B-frame can be rewritten as follows:

$$\boldsymbol{\tau}^B = \begin{bmatrix} \tau_\phi \\ \tau_\theta \\ \tau_\psi \end{bmatrix} = \begin{bmatrix} (f_2 - f_1)l_1 \\ f_3 l_3 \cos\alpha - (f_1 + f_2)l_2 \\ -f_3 l_3 \sin\alpha + \tau_3 \sin\alpha - \tau_2 + \tau_1 \end{bmatrix} \tag{2.17}$$

$$\mathbf{F}^B = \begin{bmatrix} 0 \\ -f_3 \sin\alpha + \frac{1}{l_3}(\tau_3 \cos\alpha - \tau_2 + \tau_1) \\ f_1 + f_2 + f_3 \cos\alpha \end{bmatrix} = \begin{bmatrix} 0 \\ \frac{\tau_\psi}{l_3} \\ f_1 + f_2 + f_3 \cos\alpha \end{bmatrix} \tag{2.18}$$

The tricopter dynamics system in Eq. (2.12) is presented in the B-frame. However, in this case, it can be useful to express the dynamics with respect to a composed model of linear translational equations WRT E-frame and angular equations WRT B-frame. The dynamics of the system can be rewritten as follows:

$$\begin{aligned} m\ddot{\mathbf{P}}^E &= \mathbf{F}^E = \mathbf{R}_B^E \mathbf{F}^B \\ \mathbf{J}\dot{\mathbf{\Omega}}^B + \mathbf{\Omega}^B \times \mathbf{J}\mathbf{\Omega}^B &= \boldsymbol{\tau}^B \end{aligned} \tag{2.19}$$

The Eq. (2.19) can be rewritten as follows:

$$\begin{aligned} m\ddot{x} = {} & (\cos\psi \sin\theta \sin\phi - \sin\psi \cos\phi)\frac{\tau_\psi}{l_3} \\ & +(\sin\psi \sin\phi + \cos\psi \sin\theta \cos\phi)u \end{aligned} \tag{2.20}$$

$$\begin{aligned} m\ddot{y} = {} & (\sin\psi \sin\theta \sin\phi + \cos\psi\phi \cos)\frac{\tau_\psi}{l_3} \\ & +(-\cos\psi \sin\phi + \sin\psi \sin\theta \cos\phi)u \end{aligned} \tag{2.21}$$

$$m\ddot{z} = -mg + (\cos\theta \sin\phi)\frac{\tau_\psi}{l_3} + \cos\theta \cos\phi u \tag{2.22}$$

$$I_{xx}\dot{p} = (I_{yy} - I_{zz})qr + \tau_\phi \tag{2.23}$$

$$I_{yy}\dot{q} = (I_{zz} - I_{xx})pr + \tau_\theta \tag{2.24}$$

$$I_{zz}\dot{r} = (I_{xx} - I_{yy})pq + \tau_\psi \tag{2.25}$$

where u , τ_ϕ , τ_θ and τ_ψ are the control inputs chosen to control the tricopter as:

$$u = f_1 + f_2 + f_3 \cos\alpha \tag{2.26}$$

$$\tau_\phi = (f_2 - f_1) l_1 \tag{2.27}$$

$$\tau_\theta = f_3 l_3 \cos\alpha - (f_1 + f_2) l_2 \tag{2.28}$$

$$\tau_\psi = -f_3 l_3 \sin\alpha + n(f_3 \cos\alpha - f_2 + f_1) \tag{2.29}$$

where $n = \dfrac{k_\tau}{k_f}$

Chapter 3: Controller design

The controller algorithms to control the tricopter are presented in this chapter. The dynamic modeling of the tricopter is lineared to be easier to apply the controller and reduce the algorithm complexity. The control strategy to control altitude and attitude separately is produced. The backstepping method is proposed to design the controller.

3.1 Linearization of dynamic modelling

From the previous chapter, the dynamics of the tricopter is described in the following equations:

$$m\ddot{x} = (\cos\psi\sin\theta\sin\phi - \sin\psi\cos\phi)\frac{\tau_\psi}{l_3} + (\sin\psi\sin\phi + \cos\psi\sin\theta\cos\phi)u \tag{3.1}$$

$$m\ddot{y} = (\sin\psi\sin\theta\sin\phi + \cos\psi\phi\cos)\frac{\tau_\psi}{l_3} + (-\cos\psi\sin\phi + \sin\psi\sin\theta\cos\phi)u \tag{3.2}$$

$$m\ddot{z} = -mg + (\cos\theta\sin\phi)\frac{\tau_\psi}{l_3} + \cos\theta\cos\phi u \tag{3.3}$$

$$I_{xx}\dot{p} = (I_{yy} - I_{zz})qr + \tau_\phi \tag{3.4}$$

$$I_{yy}\dot{q} = (I_{zz} - I_{xx})pr + \tau_\theta \tag{3.5}$$

$$I_{zz}\dot{r} = (I_{xx} - I_{yy})pq + \tau_\psi \tag{3.6}$$

The control inputs are u, τ_ϕ, τ_θ and τ_ψ. From Eqs. (3.1)~(3.3), all the linear translational states are subordinated to the control parameter *u*. Hence, only one state is controllable. It is to stabilize only attitude and altitude of the tricopter. Thus, the equations that describe motions of the tricopter along *x* axis and *y* axis are neglected.

Besides, the angular accelerations referred to the angles of the tricopter in B-frame are not equal to the angular acceleration of the Euler angles which determines the attitude in the E-frame. The relation between them involves the transformation matrix, **T**. Since the sensor information and actuator forces are exerted on the B-frame, so it is more natural to derive the dynamics from body-fixed velocities. Therefore, the acceleration angular equations with respect to B-frame are used to design the angular position.

Dynamic equations of the tricopter can be reduced as follows:

$$m\ddot{z} = -mg + (\cos\theta\sin\phi)\frac{\tau_\psi}{l_3} + \cos\theta\cos\phi u \tag{3.7}$$

$$\ddot{\phi} = \dot{p} = \frac{I_{yy} - I_{zz}}{I_{xx}}\dot{\theta}\dot{\psi} + \frac{\tau_\phi}{I_{xx}} \tag{3.8}$$

$$\ddot{\theta} = \dot{q} = \frac{I_{zz} - I_{xx}}{I_{yy}}\dot{\phi}\dot{\psi} + \frac{\tau_\theta}{I_{yy}} \tag{3.9}$$

$$\ddot{\psi} = \dot{r} = \frac{I_{xx} - I_{yy}}{I_{zz}}\dot{\phi}\dot{\theta} + \frac{\tau_\psi}{I_{zz}} \tag{3.10}$$

In above equations, the angular equations are still complex with the centripetal terms $(p = \dot{\phi}, q = \dot{\theta}, r = \dot{\psi})$. Therefore, a control strategy is adopted to reduce the effect of these terms. The control of the tricopter attitude is separated as shown in Fig. 3.1.

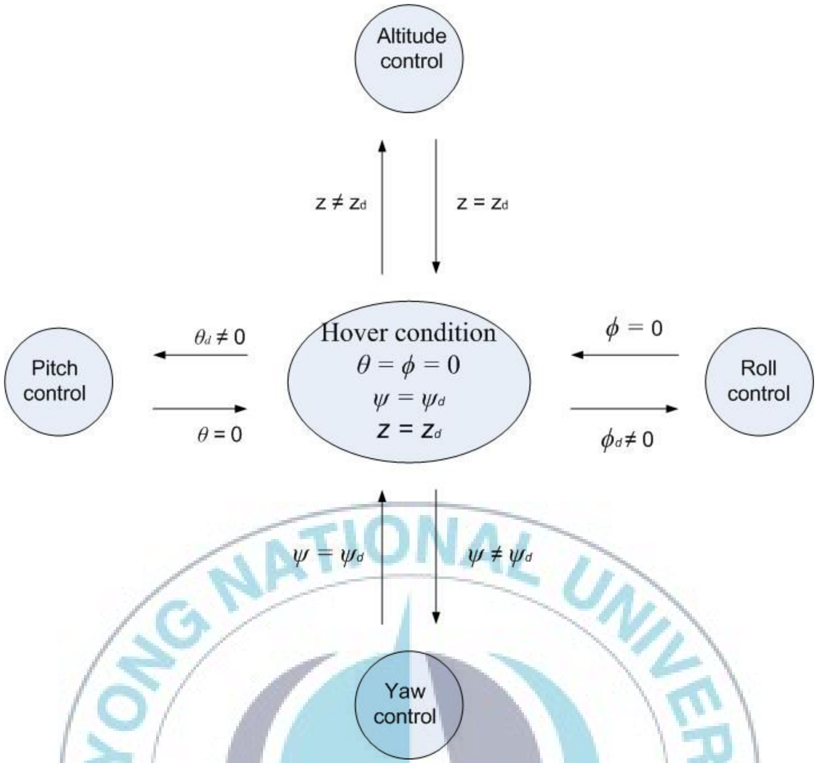

Fig. 3.1 Control strategy of the tricopter

With this strategy, each of Euler angles is controlled separately and the effects of the other Euler angles can be reduced. When altitude reference z_d is different from altitude z of the tricopter ($z \neq z_d$), the controller controls the altitude to converge to the altitude reference while roll angle ϕ and pitch angle θ stay at zero ($\phi = \theta = 0$) and yaw angle ψ does not change. When the yaw angle reference ψ_d is different from yaw angle ψ of the tricopter ($\psi \neq \psi_d$), the controller controls the yaw angle ψ to converge to the yaw angle reference ψ_d while roll angle ϕ and pitch angle θ stay at zero ($\phi = \theta = 0$ and $\dot{\phi} = \dot{\theta} = 0$). When the pitch reference θ_d is different from zero $(\theta_d \neq 0)$, the controller controls the pitch angle θ converge to the pitch reference θ_d while roll angle ϕ stay at zero $(\phi = 0)$ and yaw angle ψ does not change $(\dot{\phi} = 0, \dot{\psi} = 0)$. The control strategy for roll angle ϕ is similar as that for pitch angle θ with $(\dot{\theta} = 0, \dot{\psi} = 0)$.

The tricopter dynamics using the above control strategy is presented as follows:

$$\ddot{z} = -g + \frac{u}{m} \tag{3.11}$$

$$\ddot{\phi} = \frac{\tau_\phi}{I_{xx}} \tag{3.12}$$

$$\ddot{\theta} = \frac{\tau_\theta}{I_{yy}} \tag{3.13}$$

$$\ddot{\psi} = \frac{\tau_\psi}{I_{zz}} \tag{3.14}$$

From Eqs. (3.11)~(3.14), the actual control inputs f_1, f_2, f_3 and α can be computed as follows:

$$f_2 = \frac{1}{2}\left(\frac{l_3 u - \tau_\theta}{l_2 + l_3} + \frac{\tau_\phi}{l_1}\right) \tag{3.15}$$

$$f_1 = f_2 - \frac{\tau_\phi}{l_1} \tag{3.16}$$

$$f_3 = \sqrt{\left(u - f_1 - f_2\right)^2 + \left(\frac{n(u - 2f_2) - \tau_\psi}{l_3}\right)^2} \tag{3.17}$$

$$\alpha = \sin^{-1}\left(\frac{n(u - 2f_2) - \tau_\psi}{f_3 l_3}\right) \quad |\alpha| \leq \frac{\pi}{2} \tag{3.18}$$

Since the force generated by the tail rotor must point upwards, the angle of the tilt angle of the tail rotor is bounded as $|\alpha| \le \pi / 2$.

The transformation from ($u, \tau_\phi, \tau_\theta, \tau_\psi$) to ($f_1, f_2, f_3, \alpha$) are shown in this Appendix B.

3.2 Controller design

A tracking controller is designed using backstepping method. The objective of the tracking controller is to make altitude and attitude outputs converge to the reference altitude and attitude inputs when $t \to \infty$.

The linearized dynamic Eqs. (3.11)~(3.14) can be rewritten as follows:

$$\ddot{\mathbf{x}} = \mathbf{u} \tag{3.19}$$

$$\mathbf{x} = \begin{bmatrix} z & \phi & \theta & \psi \end{bmatrix}^T$$

$$\mathbf{u} = \begin{bmatrix} \left(-g + \dfrac{u}{m}\right) & \dfrac{\tau_\phi}{I_{xx}} & \dfrac{\tau_\theta}{I_{yy}} & \dfrac{\tau_\psi}{I_{zz}} \end{bmatrix}^T$$

State variables are defined as:

$$\begin{aligned} \mathbf{x_1} &= \mathbf{x} \\ \mathbf{x_2} &= \dot{\mathbf{x}} \end{aligned} \tag{3.20}$$

Eq. (3.19) can be presented as follows:

$$\dot{\mathbf{x}}_1 = \mathbf{x}_2$$
$$\dot{\mathbf{x}}_2 = \mathbf{u} \tag{3.21}$$

A controller is designed to make $\mathbf{x}_1$ converge to reference vector $\mathbf{x}_d = [z_d, \phi_d, \theta_d, \psi_d]^T$ when $t \to \infty$. Now, two virtual states are defined as:

$$\mathbf{z}_1 = \mathbf{x}_1 - \mathbf{x}_d \tag{3.22}$$

$$\mathbf{z}_2 = \mathbf{x}_2 - \boldsymbol{\beta} - \dot{\mathbf{x}}_d \tag{3.23}$$

From Eqs. (3.21)~(3.23), the derivatives of the virtual states $\mathbf{z}_1$ and $\mathbf{z}_2$ are derived as follows:

$$\dot{\mathbf{z}}_1 = \mathbf{x}_2 - \dot{\mathbf{x}}_d = \mathbf{z}_2 + \boldsymbol{\beta} \tag{3.24}$$

$$\dot{\mathbf{z}}_2 = \dot{\mathbf{x}}_2 - \dot{\boldsymbol{\beta}} - \ddot{\mathbf{x}}_d = \mathbf{u} - \dot{\boldsymbol{\beta}} - \ddot{\mathbf{x}}_d \tag{3.25}$$

A candidate Lyapunov function (clf) for the first virtual state is chosen as follows:

$$V_\beta = \frac{1}{2}\mathbf{z}_1^2 \tag{3.26}$$

From Eqs. (3.26) and (3.24), the derivative of the clf can be derived as follows:

$$\dot{V}_\beta = \mathbf{z}_1\dot{\mathbf{z}}_1 = \mathbf{z}_1(\mathbf{z}_2 + \boldsymbol{\beta}) \tag{3.27}$$

The virtual control $\mathbf{z}_1$ is chosen as follows:

$$\boldsymbol{\beta} = -\mathbf{K}_1\mathbf{z}_1 \tag{3.28}$$

where $\mathbf{K}_1 = diag(k_1, k_2, k_3, k_4)$ is a positive definite matrix.

Using Eq. (3.28), Eq. (3.27) becomes:

$$\dot{V}_\beta = -\mathbf{K}_1\mathbf{z}_1^2 + \mathbf{z}_1\mathbf{z}_2 \tag{3.29}$$

The above equations $\dot{V}_\beta \le 0$ does not achieve except $\mathbf{z}_1 = \mathbf{z}_2 = 0$. Now, the clf for the total system is defined as follows:

$$V = V_\beta + \frac{1}{2}\mathbf{z}_2^2 \tag{3.30}$$

From Eqs. (3.29) and (3.30), the derivative of the clf can be presented as follows:

$$\dot{V} = \dot{V}_\beta + \mathbf{z}_2\dot{\mathbf{z}}_2 = -\mathbf{K}_1\mathbf{z}_1^2 + \mathbf{z}_2(\mathbf{z}_1 + \dot{\mathbf{z}}_2) \tag{3.31}$$

Substituting Eq. (3.25) into Eq. (3.31) yields:

$$\dot{V} = -\mathbf{K}_1\mathbf{z}_1^2 + \mathbf{z}_2(\mathbf{z}_1 + \mathbf{u} - \dot{\boldsymbol{\beta}} - \ddot{\mathbf{x}}_d) \tag{3.32}$$

From above equations, the actual control is chosen to make $\dot{V} \le 0$ as follows:

$$\mathbf{u} = -\mathbf{z}_1 + \dot{\boldsymbol{\beta}} + \ddot{\mathbf{x}}_d - \mathbf{K}_2\mathbf{z}_2 \tag{3.33}$$

where $\mathbf{K}_2 = diag(k_5, k_6, k_7, k_8)$ is a positive definite matrix.

Using Eq. (3.33), Eq. (3.32) can be reduced into:

$$\dot{V} = -\mathbf{K}_1\mathbf{z}_1^2 - \mathbf{K}_2\mathbf{z}_2^2 \leq 0 \tag{3.34}$$

From Eq. (3.33), the controller designed can be derived as follows:

$$u = m\{(k_1 - k_1k_5)(z - z_d) - (k_1 + k_5)(\dot{z} - \dot{z}_d) + \ddot{z}_d + g\} \tag{3.35}$$

$$\tau_\phi = I_{xx}((k_2 - k_2k_6)(\phi - \phi_d) - (k_2 + k_6)(\dot{\phi} - \dot{\phi}_d) + \ddot{\phi}_d) \tag{3.36}$$

$$\tau_\theta = I_{yy}((k_3 - k_3k_7)(\theta - \theta_d) - (k_3 + k_7)(\dot{\theta} - \dot{\theta}_d) + \ddot{\theta}_d) \tag{3.37}$$

$$\tau_\psi = I_{zz}((k_4 - k_4k_8)(\psi - \psi_d) - (k_4 + k_8)(\dot{\psi} - \dot{\psi}_d) + \ddot{\psi}_d) \tag{3.38}$$

From Eqs. (3.24), (3.25), (3.28) and (3.33), the closed loop of the system is as follows:

$$\begin{bmatrix} \dot{\mathbf{z}}_1 \\ \dot{\mathbf{z}}_2 \end{bmatrix} = \begin{bmatrix} -\mathbf{K}_1 & 1 \\ -1 & -\mathbf{K}_2 \end{bmatrix} \begin{bmatrix} \mathbf{z}_1 \\ \mathbf{z}_2 \end{bmatrix} \tag{3.39}$$

The controller can be divided in three components as shown in Fig. 3.2.

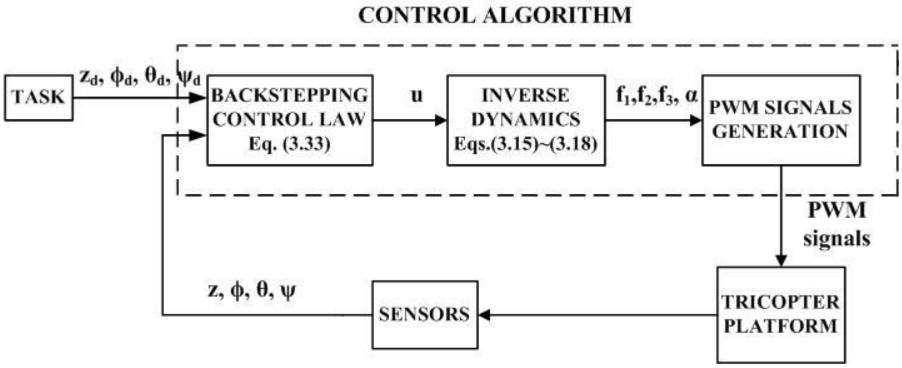

Fig. 3.2 Block diagram for the proposed controller

Chapter 4: Structure of the tricopter

This chapter describes the hardware structure of the tricopter system including actuator, sensors, hardware configuration of the control system and the software development for the MCU.

4.1 Hardware description

Fig. 4.1 shows the structure of the tricopter system used for this dissertation.

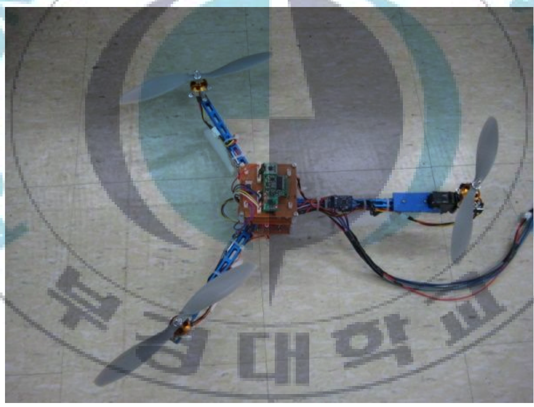

Fig. 4.1 Structure of the tricopter

The tricopter has three motors connected to the propellers and one servo motor connected to the tail motor. The two front rotors are fixed and parallel. The tail motor can tilt according to a servomechanism.

The motors used to manufacture the tricopter are the FlyCam 1400 Brushless Motor shown in Fig. 4.2. This type of motor is suitable for manufacturing tricopter. With the propeller, weight of one motor is small (43gram).

Fig. 4.2 FlyCam 1400 Brushless Motor

Each of motors connects to a propeller. When these motors rotate, the propellers rotate to drag the tricopter up. At the chapter 2, we already mentioned that the right motor and tail motor rotate clockwise and the left motor rotates counterclockwise but the forces that drag the tricopter must point upwards. Therefore, there are two types of the propeller as shown in Fig. 4.3. One type is clockwise (CW) propeller and another type is counterclockwise (CCW) propeller.

Fig. 4.3 Propeller of the tricopter

The FlyCam motor mentioned above operates with high current (4-12A). Its speed can be changed through an ESC (Electronic Speed Controller) shown in Fig. 4.4. An ESC is controlled by Pulse Width Modulation (PWM) signals from Micro Control Unit (MCU). The PWM signals vary from 1ms to 2ms at 50Hz frequency.

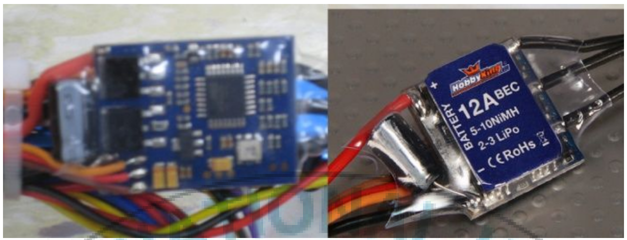

Fig. 4.4 Hobby King ESC

The tail motor can be tilted by a high torque servomotor. The servo motor shown in Fig. 4.5 is also controlled by (PWM) signals from MCU.

Fig. 4.5 Servomotor

The outputs of the tricopter system are altitude and attitude. The tricopter needs many types of sensors to get outputs' values. The tricopter's altitude is measured by a SONAR (Sountd Navigation And Ranging) sensor through ultrasound waves. The SONAR sensor communicates with the MCU through I^2C (Inter Integrated Circuit). A SONAR sensor module is shown in Fig. 4.6.

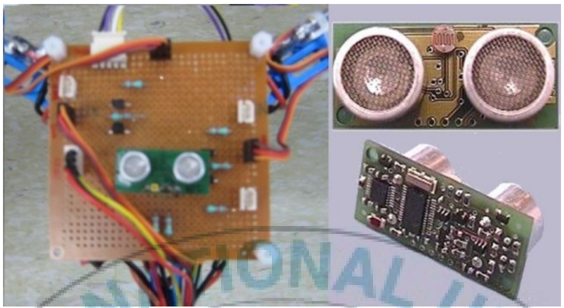

Fig. 4.6 SONAR sensor

To measure the attitude of the tricopter, three types of sensors used for the tricopter are 3-axis accelerometer, gyros sensor, and compass sensor shown in Fig. 4.7. The 3-axis accelerometer can be used to measure the pitch and roll angles. But its signal chattering behavior makes the accelerometer unreliable. Therefore, the accelerometer is implemented to compliment the gyros sensors, which measure angular velocity of the tricopter, to get more accurate angles' values. That implementation makes a complementary filter. The detail of the filter is presented in section 2. The compass sensor is used to measure the yaw angle of the tricopter. It can communicate with the MCU through I^2C or PWM.

(a) Accelerometer (b) Compass sensor (c) Gyros sensor

Fig. 4.7 Altitude measurement sensors

To control the tricopter, the MCU used for this dissertation is DSP TMS320F28335 shown in Fig. 4.8. It can be considered as the brain of the tricopter. It organizes the communication of all devices.

Fig. 4.8 Micro Control Unit

4.2 Software development

4.2.1 Software structure

The software developed is the program for the MCU. The program is loaded into the MCU. After the start-up of the system, the MCU runs the program. At first, the peripherals such as I2C, PWM, ADC (Analog Digital Converter), etc are setup to work properly. After this procedure, the main control loop begins. Each time, the program waits until the sensors finish sending the altitude and attitude data. When the sensors data are acquired, the following step is the control algorithm. It filters the sensors data to get accurate altitude and attitude values. After that, it reads the reference inputs then applies the control law to make the outputs reach the reference inputs. This phase requires a lot of computation. After computation, the appropriate PWM signals are set to the motors through ESC for controlling propellers. Then the program returns to the main control loop begins to read the sensors data again.

Fig. 4.9 shows the flow chart of the software to better understand the main control cycle.

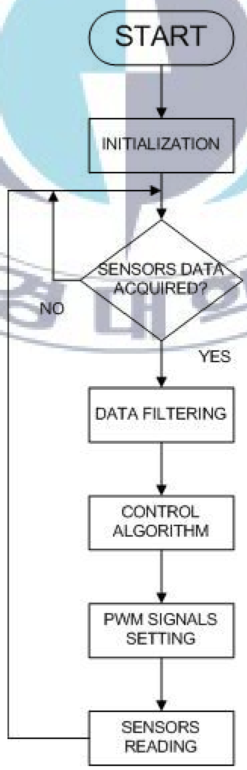

Fig. 4.9 Software flow chart

4.2.2 Complementary filter

As mentioned in section 1, accelerometer data does not always measure angle precisely. But the accelerometer data is still bounded over an extended period of time. In the other case, theoretically, the attitude of the tricopter can be calculated by integrating the angular velocities from the gyros sensors. Unfortunately, the results of integrating are not accurate because of the gyros signal noise behavior. The gyros sensors are only good for short term estimation.

Therefore, a complementary filter is implemented in software using both types of sensors to get more accurate attitude values. The idea of this filter is to apply low-pass filter for accelerometers' data and high-pass filter for the integrating of gyros sensors' data. The low-pass filter is to only pass through long-term changes and filter out short-term noise for accelerometers' data. The high-pass filter does the opposite of the low-pass filter. Since the gyros sensors are good for short term estimation, the high-pass filter is applied to pass through short-term changes of the gyros sensor's data to pass through and filter out signals with long-term changes. The complementary filter structure is shown in Fig. 4.10.

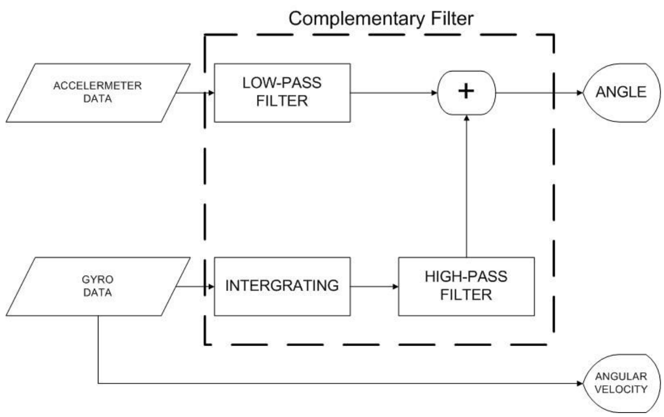

Fig. 4.10 Complementary filter structure

Chapter 5: Simulation results

Simulations is done to verify the effectiveness of the proposed controller. In the simulation, the numerical parameter values and the initial values are given in Table 5.1 and Table 5.2.

Table 5-1 Parameters' values of the tricopter

Parameters	Values	Units
l_1	0.21	m
l_2	0.12	m
l_3	0.24	m
m	0.497	kg
I_{xx}	0.0051	kgm^2
I_{yy}	0.0102	kgm^2
I_{zz}	0.0156	kgm^2

The three moments of inertia I_{xx}, I_{yy} and I_{zz} are obtained according to Appendix C.

Table 5-2 Initial Values

Parameters	Values	Units
z_0	0	m
ϕ_0	0	rad
θ_0	0	rad
ψ_0	0	rad
$f_1(0)$	0	N
$f_2(0)$	0	N
$f_3(0)$	0	N
α	0	rad
$\omega_1(0)$	0	rad/s

$\omega_2(0)$	0	*rad/s*
$\omega_3(0)$	0	*rad/s*

Table 5.3 shows the constant values for backstepping controllers.

Table 5-3 Constants' values of the controller

Constants	Values
$k_1 = k_5$	2.5
$k_2 = k_3$	5.5
$k_6 = k_7$	6.5
k_4	3
k_8	3.5

The simulation time is 20 seconds. The reference inputs are set in sequence as shown in Fig. 5.1. At first, the reference altitude is set to 0.5m. After 3 seconds, the reference yaw angle is set 50 degrees (0.872 rad). At the 6 seconds, the pitch angle reference is set 5 degrees (0.087 rad). The pitch angel reference is set zero at 8 seconds. The roll angle reference is set 10 degrees (0.174 rad) at 10 seconds. And at 12 seconds, the roll angle reference is set zero.

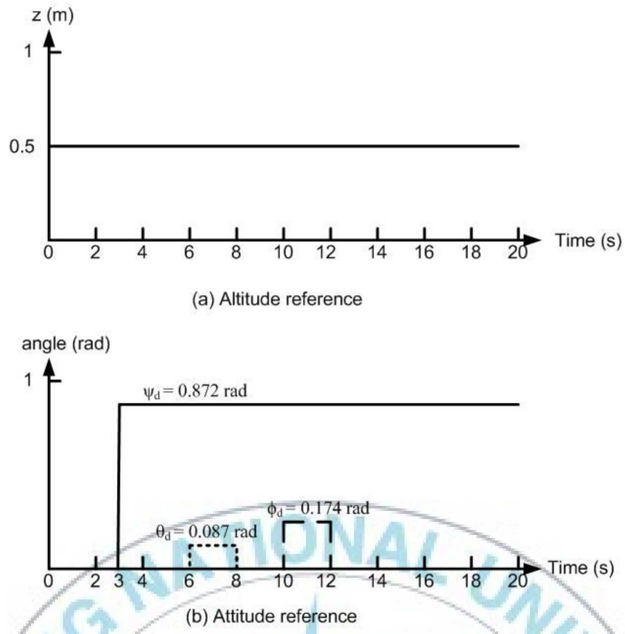

Fig. 5.1 Altitude and attitude references

5.1 Simulation results

The simulation results of the tricopter are presented in Figs. 5.2~5.5. Fig. 5.2 shows the tricopter reaches the altitude reference 0.5m in 3 seconds.

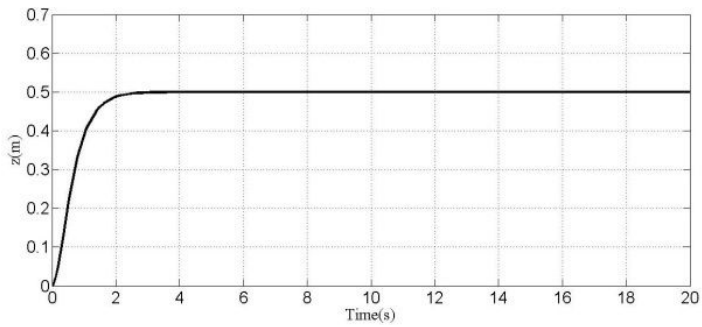

Fig. 5.2 Altitude of the tricopter

After reaching the reference altitude, the tricopter is controlled to rotate as shown in Fig. 5.3. The yaw angle reference is set to 50 degrees (0.872 rad) at 3 seconds. The yaw angle converges to reference at 50 degrees after 2 seconds. The pitch angle reference is set 5 degrees (0.087rad) at 6 seconds. The pitch angle converges to reference at 5 degrees after 1 second. The roll angle reference is set 10 degrees (0.174 rad) at 10 seconds. The roll angle converges to reference at 10 degrees after 1 second.

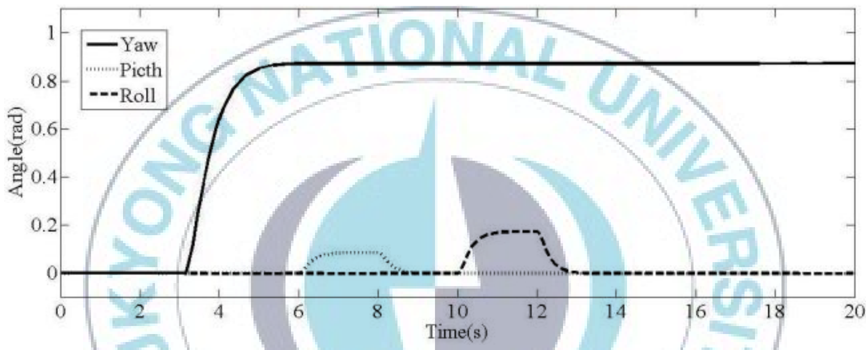

Fig. 5.3 Attitude of the tricopter

Altitude error of the tricopter is shown in Fig. 5.4. The altitude error converges to zero in 3 seconds.

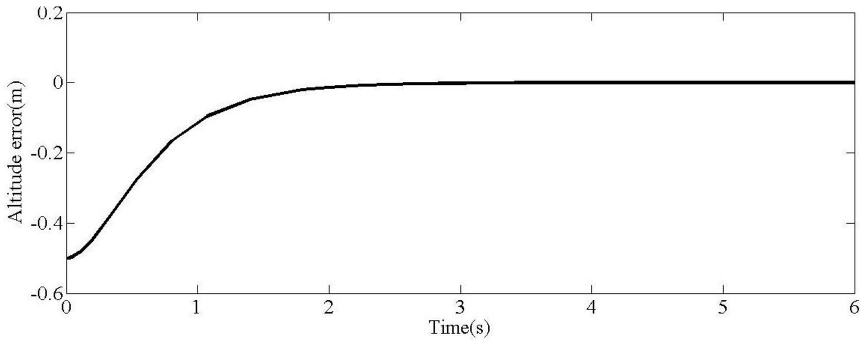

Fig. 5.4 Altitude error of the tricopter

Fig 5.5 shows the attitude errors of the tricopter. The yaw angle reference is set to 50 degrees (0.872 rad) at 3 seconds. The yaw angle error equals -0.872 rad and then converges to zero after 2 seconds. The pitch angle reference is set 5 degrees (0.087 rad) at 6 seconds. The pitch angle error equals -0.087 rad and then converges to zero after 1 second. The pitch angle reference is set zero at 8 seconds. The pitch angle error equals 0.087 rad and then converges to zero after 1 second. The roll angle reference is set 10 degrees (0.174 rad) at 10 seconds. The roll angle error equals -0.174 rad and then converges to zero after 1 second. The roll angle reference is set zero at 12 seconds. The roll angle error equals 0.174 rad and then converges to zero after 1 second.

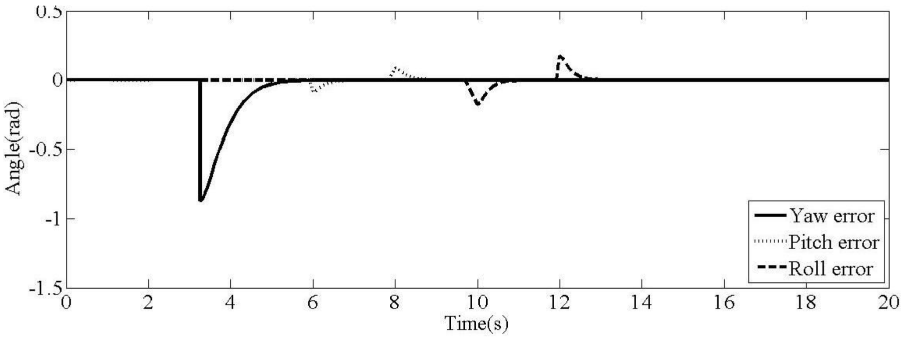

Fig. 5.5 Attitude errors of the tricopter

The chosen control inputs are shown in Fig. 5.6 and Fig. 5.7. At first, the total thrust of the tricopter increases to 7 N to make the tricopter take off. Then, the total thrust decreases to 5N to compensate the gravity force on tricopter and keeps the tricopter at altitude 0.5 m.

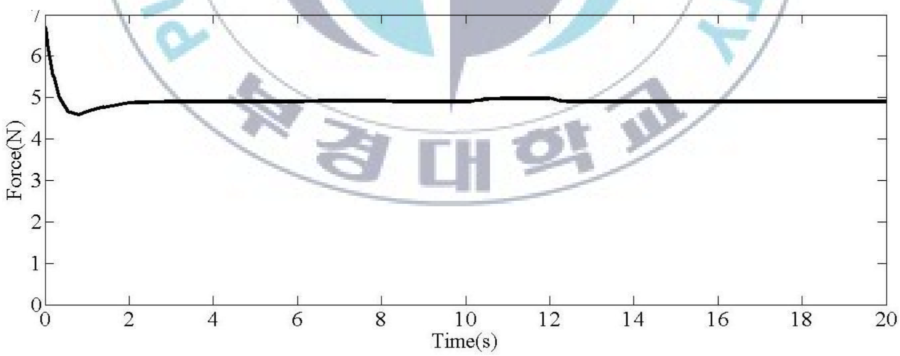

Fig. 5.6 Total thrust of the tricopter (u)

In Fig. 5.7, the yaw torque increases to 0.2 Nm at 3 seconds to make the tricopter rotate CCW about z axis. Then the torque converges to zero fast to keep the tricopter not rotate about z axis. At

6 seconds, the pitch torque increases to 0.15 Nm to make the tricopter rotate CCW about *y* axis. Then the torque converges to zero fast to keep the tricopter not rotate about *y* axis and keep pitch angle not change. At 8 seconds, the pitch torque decreases to -0.15 Nm to make the tricopter rotate CW about *y* axis. Then the torque converges to zero fast to keep the tricopter not rotate about *y* axis and keep pitch angle not change. At 10 seconds, the roll torque increases to 0.1 Nm to make the tricopter rotate CCW about *x* axis. Then the torque converges to zero fast to keep the tricopter not rotate about *x* axis and keep roll angle not change. At 12 seconds, the pitch torque decreases to -0.15 Nm to make the tricopter rotate CW about *x* axis. Then the torque converges to zero fast to keep the tricopter not rotate about *x* axis and keep roll angle not change.

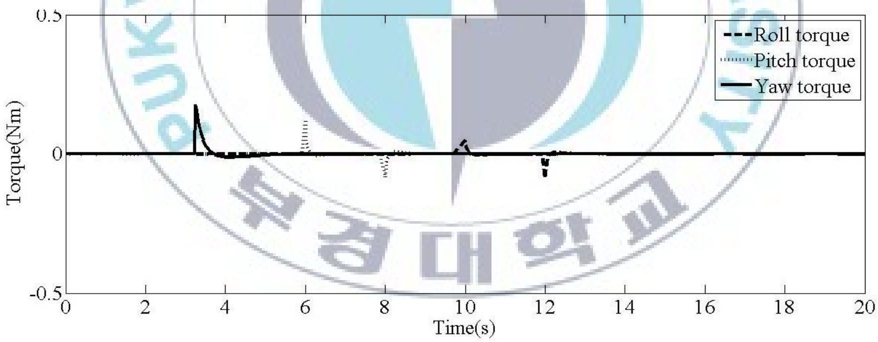

Fig. 5.7 Torques of the tricopter ($\boldsymbol{\tau}$)

Fig. 5.8 shows the angle of the tail motor. At about 3 seconds, it has sudden changes and returns to 0.1 rad (≈ 6 degrees) rapidly.

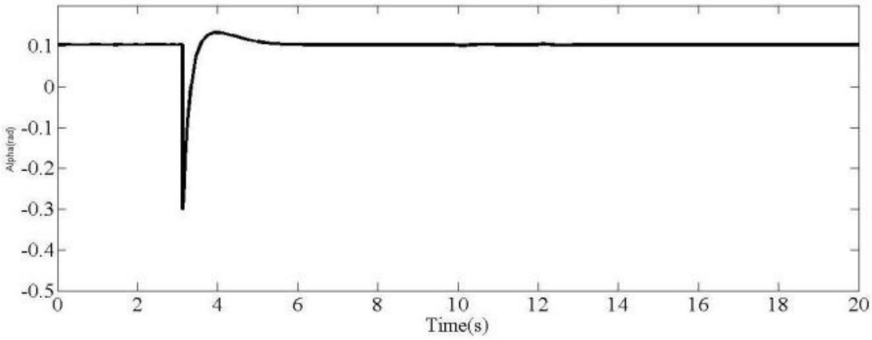

Fig. 5.8 Angle of the tail motor

In Fig. 5.9, the forces of the rotors are shown. These forces are equal to each other to keep the tricopter in balance.

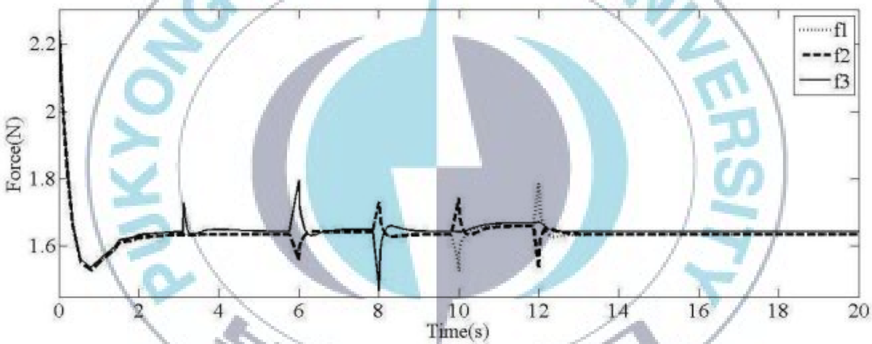

Fig. 5.9 Forces of the rotors

The forces have sudden sharp edges when the altitude of the tricopter is changed and rapidly converge to some constants values of about 1.6 N to stabilize the tricopter. At the beginning, three forces of the rotors are increased and decreased, then converge to some constants to make the tricopter reach the altitude reference and stay at that position. At the 3 seconds, the force and the tilting angle of the tail rotor (rotor 3) are changed and then converge to some constants (≈1.6 N, ≈0.1 rad). These actions are to make the yaw movement reach the yaw reference. At the 6 seconds, the force of rotor 3 is increased and the forces of rotor 1 (front right rotor) and 2 (front left rotor) are decreased to make pitch movement reach the pitch reference and then converged to some constants (≈1.6 N). At the 8 seconds, the force of rotor 3 is decreased and the forces of rotor 1 and 2 are increased to make pitch movement reach zero and then converge to some constants (≈1.6 N). At 10 seconds, the force of rotor 3 does not change, the force of rotor 2 is increased, the force of rotor 1 is decreased to make roll movement reach the roll reference and then these three forces converge to some constants (≈1.6 N).

Chapter 6: Conclusions and future works

6.1 Conclusions

This dissertation is about controlling a three rotor helicopter. The conclusions of this dissertation are summarized as follows:

- Kinematic and dynamic modellings of the tricopter are presented. The Newton-Euler formula and the Euler angles theories are used to provide the modellings information with physics and mathematical derivatives. The dynamic modelling is linearized to reduce its complexity.
- A control strategy to control the altitude and attitude separately is proposed. From the linearized dynamic model and the control strategy, a tracking controller is designed using the backstepping control algorithm.

- A real tricopter platform is developed with several interconnected devices such as motors, sensors, (MCU), etc. The software for the MCU is developed to filter the sensors' data and handle the control algorithm which provides the signals to the motors.
- The simulation results show that the outputs converge to the reference inputs rapidly with appropriate value of the forces on the tricopter. The outputs converges to the references inputs rapidly. The tricoter reaches the altitude reference 0.5 m in 3 seconds. After reaching the reference altitude, the yaw angle converges to its reference of 50 degrees after 2 seconds. The pitch angle converges to its reference of 5 degrees after 1 second. The roll angle converges to its reference of 10 degrees after 1 second. They verify the effectiveness of the proposed controller.

6.2 Future works

The proposed controller in this dissertation was based on the linearized dynamics model. There are a lot of nonlinear terms neglected. Therefore, the performance of the system is limited. To improve its performance, a new control method should be developed.

This dissertation only considered altitude and attitude control of the tricopter. But a tricopter needs to move correctly to any directions. Therefore, a controller to control the translational positions of the tricopter must be considered.

References

[1] A. Dzul, P. Castillo and R. Lozano, " *Real-time Stabilization and Tracking of a Four-rotor Mini Rotorcraft*", IEEE Transaction on Control System Technology, Vol. 12, pp. 510-516, 2004.

[2] R. Lozano, P. Castillo and A. Dzul, "*Stabilization of a Mini Rotorcraft Having Four Rotors*", Proceedings of 2004 IEEE/RSJ International Conference on Intelligent Robots and Systems, pp. 2693-2698, 2004.

[3] A. Palomino, S. Salazar-Cruz and R. Lozano, "*Trajectory Tracking for a Four Rotor Mini-aircraft*", Proceedings of the 44th IEEE Conference on Decision and Control, and the European Control Conference 2005, pp. 2505-2510, 2005.

[4] R. Lozano, P. Castillo and A. Dzul, "*Stabilization of a Mini Rotorcraft with Four Rotors*", IEEE Control Systems Magazine, pp.45-55, 2005.

[5] S. Salazar-Cruz, F. Kendoul, R. Lozano and I. Fantoni, "*Real-Time Stabilization of a Small Three-Rotor Aircraft*", IEEE Transactions on Aerospace and Electronic Systems, Vol. 44, pp. 783-749, 2008.

[6] D.W. Yoo, H.D. Oh, D.Y. Won and M.J. Tahk, "*Dynamic Modeling and Stabilization Techniques for Tri-rotor Unmanned*

Aerial Vehicles", Int'l J. of Aeronautical & Space Sci, Vol. 11, pp. 167-174, 2010.

[7] H. Romero, S. Salazar and R. Lozano, "*Real-Time Stabilization of an Eight-Rotor UAV Using Optical Flow*", IEEE Transactions on Robotics, Vol. 25, pp. 809-817, 2009.

[8] J. Kim, M.S. Kang and S. Park, "*Accurate Modeling and Robust Hovering Control for a Quad-rotor VTOL Aircraft*", Journal of Intelligent & Robotic Systems, Vol. 57, pp. 9-26, 2010.

[9] F. Kendoul, I. Fantoni and R. Lozano, "*Modeling and Control of a Small Autonomous Aircraft Having Two Tilting Rotors*", IEEE Transactions on Robotics, Vol. 22, pp. 1297-1302, 2006.

[10] J. A. Vilchis, B. Brogliato, A. Dzul and R. Lozano, "*Nonlinear Modeling and Control of Helicopters*", Automatica, Vol. 39, pp. 1583-1596, 2003.

[11] R. W. Pouty, "*Helicopter Performance, Stability and Control*", K. P. Company, Florida, 1995.

[12] W. Johnson, "*Helicopter Theory*", N. P. U. P. Princeton, New Jersey, 1980.

[13] G. Buskey, G. Wyeth and J. Roberts, "*Autonomous Helicopter Hover Using an Artificial Neutral Network*", Proceedings of the IEEE International Conference on Robotics and Automation, Seoul, Korea, pp. 1635-1640, 2001.

[14] H. Shim, T. J. Koo, F. Hoffman and S. Sastry, "*A Comprehensive Study of Control Design of an Autonomous Helicopter*", Proceedings of the 37th IEEE Conference on Decision and Control, pp. 3653-3658, 1998.

[15] S. Bouabdallah and R. Siegwart, "*Backstepping and Sliding-mode Techniques Applied to an Indoor Micro Quadrotor*", Proceedings of the IEEE International Conference on Robotics and Automation, Barcelona, Spain, pp. 2259-2264, 2005.

[16] E. N. Johnson and S. K. Kannan, "*Adaptive Flight Control for an Autonomous Unmanned Helicopter*", AIAA Guidance, Navigation and Control Conference, paper AIAA-2002-4439, 2002.

[17] T. Lauvdal and R. M. Murray, "*Stabilization of a Pitch Axis Flight Control Experiment with Input Rate Saturation*", Modeling, Identification and Control, Vol. 20, pp.225-240, 1999.

[18] J. H. Sussmann, D. E. Sontag and Y. Yang, "*A General Result on the Stabilization of Linear Systems Using Bounded Controls*", IEEE Transactions on Automatic Control, Vol. 39, pp. 2411-2425, 1994.

[19] L. Beji and A. Abichou, "*Trajectory Generation and Tracking of a Mini-rotorcraft*", Proceedings of the International Conference on Robotics and Automation, Barcelona, Spain, pp. 2629-2634, 2005.

[20] A. Tayebi and S. McGilvray, "*Attitude Stabilization of a Four-Rotor Aerial Robot*", 43rd IEEE Conference on Decision and Control, Atlantis, Paradise Island, Bahamas, pp.1216-1221, 2004.

[21] A. Dzul, R. Lozano and P. Castillo, "*Adaptive Control for a Radio-controlled Helicopter in a Vertical Flying Stand*", International Journal of Adaptive Control and Signal Processing, Vol. 18, pp. 473-485, 2004.

[22] D. Lyon, "*A military Perspective on Small Unmanned Aerial Vehicles*", IEEE Instrumentation and Measurement Magazine, Vol. 7, pp. 27-31, 2004.

[23] T. S. Alderete, "*Simulator Aero Model Implementation*", NASA Ames Research Center, Vol. 34, pp. 33-49, 1995.

[24] L. Muratet, S. Doncieux, Y. Brière and J. A. Meyer, "*A Contribution to Vision-based Autonomous Helicopter Flight in Urban Environment*", Robotics and Autonomous Systems, Vol. 50, pp. 195-209, 2005.

[25] K. Tanaka, H. Ohtake and H. Wang, "*A Practical Design Approach to Stabilization of a 3-DOF RC Helicopter*", IEEE Transactions on Automatic Control, Vol. 12, pp.315-325.

[26] S. Salazar-Cruz and R. Lozano, "*Stabilization and Nonlinear Control for a Novel Trirotor Mini-aircraft*", Proceedings of the 2005 IEEE International Conference on Robotics and Automation, pp. 2612-2617, 2005.

[27] A. Tayebi and S. McGilvray, "*Attitude Stabilization of a VTOL Quadrotor Aircraft*", IEEE Transaction on Control System Technology, Vol. 14, pp. 562-571, 2006.

[28] S. Bouabdalah, A. Noth and R. Siegwart, "*PID vs LQ Control Techniques Applied to an Indoor Micro Quadrotor*", Proceedings 2004 IEEE/RSJ International Conference on Intelligent Robots and Systems, Vol. 3, pp. 2451-2456, 2004.

[29] Y. Morel and A. Leonessa, "*Direct Adaptive Tracking Control of Quadrotor Aerial Vehicles*", Florida Conference on Recent Advances in Robotics, pp.1-6, 2006.

[30] A. Mokhtary and A. Benallegue, "*Dynamic Feedback Controller of Euler Angles and Wind Parameters Estimation for a Quadrotor Unmanned Aerial Vehicle*", Proceedings of the 2004 IEEE International Conference on Robotics and Automation, pp. 2359-2366, 2004.

[31] A. Bernallegue, V. Mister and N. K. M'Sirdi, "*Exact Linearization and Non-interacting Control of a 4 Rotor Helicopter via Dynamic Feedback*", IEEE International Workshop on Robot and Human Interactive Communication, pp. 586-593, 2001.

[32] T. Hamel, N. Geunard and R. Mhony, "*A Practical Visual Servo Control for a Unmanned Aerial Vehicle*", 2007 IEEE International Conference on Robotics and Automation, pp. 1342-1248, 2007.

[33] T. Hamel, N. Metni and F. Derkx, "*Visual Tracking Control of Aerial Robotic Systems with Adaptive Depth Estimation*", Proceedings of the 44th IEEE Conference on Decision and Control, pp. 6078-6084, 2005.

[34] J. P. Ostrowski, E. Altug and C. J. Taylor, "*Quadrotor Control Using Dual Camera Visual Feedback*", Proceedings of the 2003 IEEE International Conference on Robotics and Automation, pp. 3956-3961, 2004.

[35] C. Coza and C. J. B. Macnab, "*A New Robust Adaptive-fuzzy Control Method Applied to Quadrotor Helicopter Stabilization*" Annual meeting of the North American, Fuzzy Information Processing Society, 2006.

[36] M. Tarbouchi, J. Dunfied and G. Labonte, "*Neural Network Based Control of a Four Rotor Helicopter*", 2004 IEEE International Conference on Industrial Technology, pp. 1543-1548, 2004.

[37] S. Salazar-Cruz, H. Romero, R. Lozano and P. Castillo, "*Modeling and Real-Time Stabilization of an Aircraft Having Eight Rotors*", Journal of Intelligent & Robotic Systems, Vol. 54, pp. 455-470, 2009.

[38] A. R. Teel, "*Global Stabilization and Restricted Tracking for Multiple Integrators with Bounded Controls*", Systems and Control Letters, Vol. 18, pp. 165-171, 1992

[39] http://en.wikipedia.org/wiki/Unmanned_aerial_vehicle

[40] http://www.mathworks.com

[41] http://www.ti.com

Publications and Conferences

[1] Gyeong Mok Lee, Giang Hoang, Tan Tung Phan, Hak Kyeong Kim, Sang Bong Kim, "*Control of Omini-Directional Mobile Vehicle for Obstacle Avoidance*", Proceedings of The 1st International Symposium on Automotive & Convergence Engineering, pp. 150-158, 2011

[2] Viet Tuan Dinh, Giang Hoang, Van Giap Nguyen, Hak Kyeong Kim and Sang Bong Kim, "*Optimal Controller Design for Mobile Inverted Pendulum*", Proceedings of The 1st International Symposium on Automotive & Convergence Engineering, pp. 213-217, 2011

[3] Viet Tuan Dinh, Giang Hoang, Thien Phuc Tran, Hak Kyeong Kim and Sang Bong Kim, "*Motion Control of Omnidirectional Mobile Platform for Path Following Using Backstepping Technique*", Proceedings of The 1st International Symposium on Automotive & Convergence Engineering, pp. 55-59, 2011

[4] Giang Hoang, Viet Tuan Dinh, Hak Kyeong Kim, Van Giap Nguyen and Sang Bong Kim, "*Altitude and Attitude Control of a Three Rotor Helicopter*", Proceedings of The 2011 International Symposium on Advanced Engineering, pp. 127-133, 2011

Appendix A

From Fig. 2.5, the following vectors are derived as follow:

$$\begin{aligned}
\overrightarrow{GR_1} &= (l_2, -l_1, 0) \\
\overrightarrow{GR_2} &= (l_2, l_1, 0) \\
\overrightarrow{GR_3} &= (-l_3, 0, 0,)
\end{aligned} \tag{A.1}$$

From Eqs. (2.14) and (A.1), the torque vector on tricopter in B-frame, $\boldsymbol{\tau}^B$, is derived as follows:

$$\begin{aligned}
(\boldsymbol{\tau}^B)^T &= (l_2, -l_1, 0) \times \left(0, 0, f_1\right) + (l_2, l_1, 0) \times \left(0, 0, f_2\right) \\
&\quad + (-l_3, 0, 0) \times \left(0, f_3 \sin\alpha, f_3 \cos\alpha\right)
\end{aligned} \tag{A.2}$$

From the above equation, $\boldsymbol{\tau}^B$ is rewritten as follows:

$$\begin{aligned}
(\boldsymbol{\tau}^B)^T &= (-l_1 f_1, -l_2 f_1, 0) + (l_1 f_2, -l_2 f_2, 0) + \left(0, f_3 l_3 \cos\alpha, -f_3 l_3 \sin\alpha\right) \\
\Rightarrow \boldsymbol{\tau}^B &= \begin{pmatrix} -l_1 f_1 \\ -l_2 f_1 \\ 0 \end{pmatrix} + \begin{pmatrix} l_1 f_2 \\ -l_2 f_2 \\ 0 \end{pmatrix} + \begin{pmatrix} 0 \\ f_3 l_3 \cos\alpha \\ -f_3 l_3 \sin\alpha \end{pmatrix} \\
&= \begin{pmatrix} (f_2 - f_1) l_1 \\ f_3 l_3 \cos\alpha - (f_1 + f_2) l_2 \\ -f_3 l_3 \sin\alpha \end{pmatrix}
\end{aligned}$$

Appendix B

Transformations from ($u,\tau_{\phi},\tau_{\theta},\tau_{\psi}$) to (f_1,f_2,f_3,α) are shown in this appendix. For every ($u,\tau_{\phi},\tau_{\theta},\tau_{\psi}$), there exists one and only one (f_1,f_2,f_3,α).

From Eqs. (2.26)~(2.28), the following equations are derived as:

$$f_2 - f_1 = \frac{\tau_{\phi}}{l_1} \tag{B.1}$$

$$f_1 + f_2 = \frac{f_3 l_3 \cos\alpha - \tau_{\theta}}{l_2} \tag{B.2}$$

$$f_3 \cos\alpha = u - (f_1 + f_2) \tag{B.3}$$

Substituting Eq. (B.3) into Eq. (B.2), the following equation is derived as:

$$f_1 + f_2 = \left(\frac{1}{l_2 + l_3}\right)\left(l_3 u - \tau_{\theta}\right) \tag{B.4}$$

Adding Eq. (B.1) and Eq. (B.4), f_2 is derived as follows:

$$f_2 = \frac{1}{2}\left(\frac{l_3 u - \tau_{\theta}}{l_2 + l_3} + \frac{\tau_{\phi}}{l_1}\right) \tag{B.5}$$

From Eq. (B.1), f_1 can be reduced as following equation:

$$f_1 = f_2 - \frac{\tau_\phi}{l_1} \tag{B.6}$$

From Eq. (2.29) and Eq. (2.26), the following equation is derived as:

$$f_3 \sin\alpha = \frac{1}{l_3}\left(n\left(u - 2f_2\right) - \tau_\psi\right) \tag{B.7}$$

From Eq. (B.3) and Eq. (B.7), f_3 is derived as follows:

$$f_3 = \sqrt{\left(u - f_1 - f_2\right)^2 + \frac{1}{l_3^2}\left(n\left(u - 2f_2\right) - \tau_\psi\right)^2} \tag{B.8}$$

And tilt angle of the tail rotor can be derived from Eq. (B.7) as follows:

$$\alpha = \sin^{-1}\left(\frac{1}{f_3 l_3}\left(n\left(u - 2f_2\right) - \tau_\psi\right)\right) \tag{B.9}$$

Since the force generated by the tail rotor must point upwards, the angle of the tilt angle of the tail rotor is bounded as: $\left|\alpha\right| \le \pi / 2$.

Appendix C

In the tricopter's body moment of inertia calculation, the main task is to identify the dynamic behavior of the tricopter in rotation around a defined axis. The three moments of inertia I_{xx}, I_{yy} and I_{zz} are derived in two steps.

Step 1:

The structure of the tricopter is modeled as several components with simpler geometry as follows:

- 3 motors are modeled as solid cylinders
- Servo motor is modeled as a rectangular parallelepiped
- Sensors box is modeled as a rectangular parallelepiped

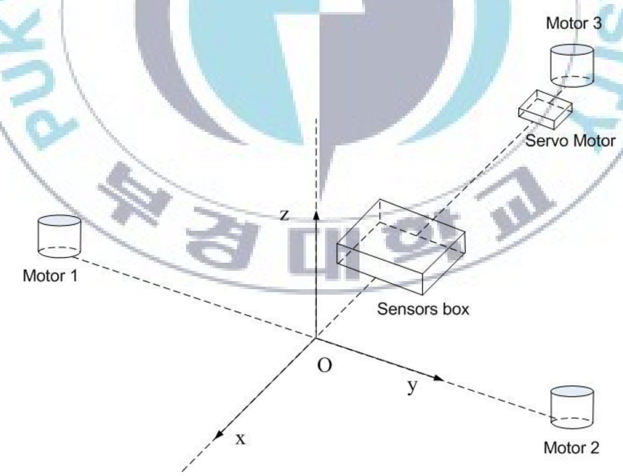

Fig. C.1 Geometric modeling of the tricopter

Step 2:

The moments of inertia around the x axis, y axis and z axis of each component are calculated.

The rectangular parallelepiped of the sensors box has a length L_B, a width W_B, a height H_B, a mass M_B, the distances from center of gravity of the sensors box to *x* axis, *y* axis and *z* axis, D_{Bx}, D_{By} and D_{Bz}, respectively.

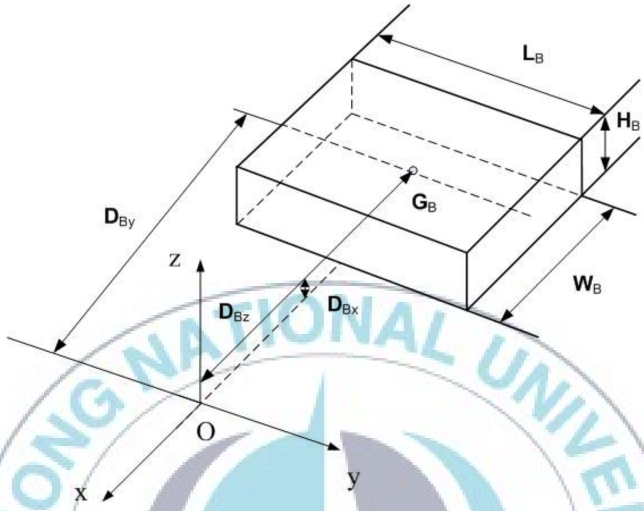

Fig. C.2 Sensors box geometry

The moments of inertia of the sensors box around the *x* axis, *y* axis and *z* axis, I_{Bx}, I_{By} and I_{Bz}, are derived by definition of scalar moment of inertia and parallel axes theorem. The moments of inertia of the sensors box can be calculated as follows:

$$I_{Bx} = \mathrm{M_B}\left(\frac{\mathrm{W_B^2}}{12} + \frac{\mathrm{H_B^2}}{12} + \mathrm{D_{Bx}^2}\right) \tag{C.1}$$

$$I_{By} = \mathrm{M_B}\left(\frac{\mathrm{L_B^2}}{12} + \frac{\mathrm{H_B^2}}{12} + \mathrm{D_{By}^2}\right) \tag{C.2}$$

$$I_{Bz} = \mathrm{M_B}\left(\frac{\mathrm{W_B^2}}{12} + \frac{\mathrm{L_b^2}}{12} + \mathrm{D_{Bz}^2}\right) \tag{C.3}$$

The servo motor model is also rectangular parallelepiped. Similarly, the moments of inertia of the servo motor around the *x* axis, *y* axis and *z* axis, I_{Sx}, I_{Sy} and I_{Sz} are calculated as follows:

$$I_{Sx} = \mathrm{M_S}(\frac{\mathrm{W_S^2}}{12} + \frac{\mathrm{H_S^2}}{12} + \mathrm{D_{Sx}^2}) \tag{C.4}$$

$$I_{Sy} = \mathrm{M_S}(\frac{\mathrm{L_S^2}}{12} + \frac{\mathrm{H_S^2}}{12} + \mathrm{D_{Sy}^2}) \tag{C.5}$$

$$I_{Sz} = \mathrm{M_S}(\frac{\mathrm{W_S^2}}{12} + \frac{\mathrm{L_S^2}}{12} + \mathrm{D_{Sz}^2}) \tag{C.6}$$

The rectangular parallelepiped of the servo motor has a length $\mathrm{L_S}$, a width $\mathrm{W_S}$ a height $\mathrm{H_S}$, a mass $\mathrm{M_S}$ and the distances from center of gravity of the servo motor to x axis, y axis and z axis, $\mathrm{D_{Sx}}$, $\mathrm{D_{Sy}}$ and $\mathrm{D_{Sz}}$, respectively.

The solid cylinder of the i^{th} motor model has a radius $\mathrm{R}_{\mathrm{M}i}$, a height $\mathrm{H}_{\mathrm{M}i}$, a mass $\mathrm{M}_{\mathrm{M}i}$ and the distances from center of gravity of the motor to *x* axis, *y* axis and *z* axis, $\mathrm{D}_{\mathrm{M}ix}$, $\mathrm{D}_{\mathrm{M}iy}$ and $\mathrm{D}_{\mathrm{M}iz}$, respectively. ($i$ = 1,2,3)

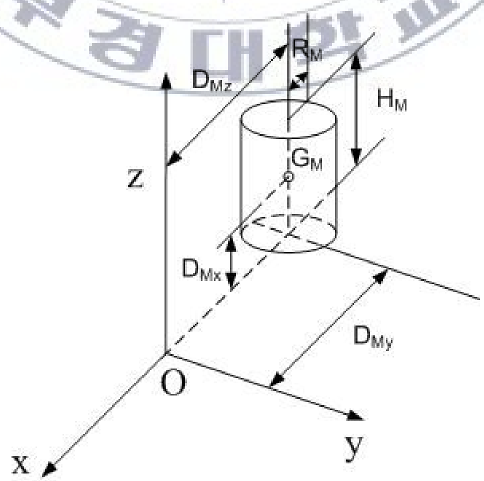

Fig. C.3 Motor geometry

The moments of inertia of the motor around the x axis, y axis and z axis, I_{Mix}, I_{Miy} and I_{Miz} can be calculated as follows:

$$I_{Mix} = \mathrm{M}_{\mathrm{M}i}\left(\frac{\mathrm{R}_{\mathrm{M}i}^2}{4} + \frac{\mathrm{H}_{\mathrm{M}i}^2}{12} + \mathrm{D}_{\mathrm{M}ix}^2\right) \tag{C.7}$$

$$I_{Miy} = \mathrm{M}_{\mathrm{M}i}\left(\frac{\mathrm{R}_{\mathrm{M}i}^2}{4} + \frac{\mathrm{H}_{\mathrm{M}i}^2}{12} + \mathrm{D}_{\mathrm{M}iy}^2\right) \tag{C.8}$$

$$I_{Miz} = \mathrm{M}_{\mathrm{M}i}\left(\frac{\mathrm{R}_{\mathrm{M}i}^2}{2} + \mathrm{D}_{\mathrm{M}iz}^2\right) \tag{C.9}$$

Using above equations, the moments of inertia of the three motors can be calculated.

Finally, the tricopter moments of inertia I_{xx}, I_{yy} and I_{zz} can be calculated by adding all the components around x axis, y axis and z axis, respectively.

$$I_{xx} = I_{Bx} + I_{Sx} + I_{M1x} + I_{M2x} + I_{M3x} \tag{C.10}$$

$$I_{yy} = I_{By} + I_{Sy} + I_{M1y} + I_{M2y} + I_{M3y} \tag{C.11}$$

$$I_{zz} = I_{Bz} + I_{Sz} + I_{M1z} + I_{M2z} + I_{M3z} \tag{C.12}$$

where I_{Mij} is moment of inertia of i^{th} motor around axis j, for $i = (1,2,3)$ and $j = (x, y, z)$.

Table C-1 Parameters for moment of inertia calculation

Parameters	**Values**	**Units**
M_B	0.32	*kg*
W_B	0.08	*m*
H_B	0.1	*m*
L_B	0.08	*m*
D_{Bx}	0.05	*m*
D_{By}	0.12	*m*
D_{Bz}	0.13	*m*
M_S	0.045	*kg*
W_S	0.036	*m*
H_S	0.02	*m*
L_S	0.04	*m*
D_{Sx}	0.013	*m*
D_{Sy}	0.24	*m*
D_{Sz}	0.24	*m*
M_i	0.043	*kg*
R_i	0.014	*m*
H_i	0.026	*m*
D_{M1x}	0.21	*m*
D_{M1y}	0.013	*m*
D_{M1z}	0.24	*m*
D_{M2x}	0.21	*m*
D_{M2y}	0.013	*m*
D_{M2z}	0.24	*m*
D_{M3x}	0.013	*m*
D_{M3y}	0.24	*m*
D_{M3z}	0.24	*m*